Modelling Turbine Loads during an Extreme Coherent Gust using Large Eddy Simulation

R. C. Storey[1], S. E. Norris[2] and J. E. Cater[1]
[1]**Department of Engineering Science, The University of Auckland, New Zealand**
[2]**Department of Mechanical Engineering, The University of Auckland, New Zealand**

Abstract. A group of wind turbines operating in extreme transient wind conditions has been simulated using LES and an actuator model. An extreme wind event is introduced into the simulation domain using transient boundary conditions. The event is based on the extreme coherent gust (ECG) structure from the International Wind Turbine Design Standard IEC61400-1:2005 which consists of a simultaneous gust and wind direction change. Details of the implementation are discussed with regard to adapting the analytical functions described in the standard. A recently developed actuator sector method is used to represent the wind turbines in the simulation. The actuator method is coupled to the aero-elastic wind turbine simulation code FAST to allow dynamic control of the wind turbines based on the ambient flow conditions. Standard baseline controllers are used to regulate generator torque, actuate blade pitch angle and control yaw direction. A span-wise periodic array of turbines operating in a steady atmospheric boundary layer is simulated before the introduction of the ECG structure. The convection of the wind event is analysed, along with the subsequent response of the wind turbines and loading during the wind event is quantified. The simulations demonstrate a methodology for modelling groups of turbines operating in transient wind conditions that can be used to study turbine loads or test new turbine control strategies.

1. Introduction

Analysis of wind turbine operation and loading requires modelling of the dynamics of the wind turbine plant as well as the wind environment to which the turbine is responding. The latter presents several modelling challenges due to its transient nature and complex structure. Although a wind turbine operating in a steady onset flow is of interest, a more comprehensive analysis of a wind turbine design involves the examination of turbine responses to larger scale turbulence structures such as large gusts and rapid wind direction changes. For example, a set of extreme wind events is presented in the International Wind Turbine Design Standard IEC61400-1:2005 [1].

Variations in wind speed and direction can be modelled using techniques such as synthetic turbulence generation, e.g. Mann [2], where an inverse Fourier transform method is used to generate a set of turbulent fluctuations with a specified shear, length scale, and intensity. This method can be applied in a computational fluid dynamics (CFD) based simulation where a wind environment is modelled using a specified inlet velocity profile at with the turbulent fluctuations superimposed [3]. Introducing a large wavelength or amplitude turbulence structure is also possible using this method, however control over the resulting flow field is limited. An alternative is to develop a wind event structure in a CFD simulation using a carefully constructed set of boundary conditions. This technique has been successfully implemented in a large eddy simulation (LES) by Norris et. al.[4, 5] where a 3-D gust structure was modelled.

In addition to modelling turbulent structures in the ABL, the effect of the wind turbine itself should be taken into account in the modelling of the flow physics. This is especially important for locations where the free-stream flow upwind of a turbine is affected by neighbouring turbine wakes. This scenario is common where groups of turbines are arranged to utilise available land and regions with high wind resources [6]. In offshore environments in particular, regular arrays of turbines are often used. Wake

regions, characterised by a velocity deficit and increased turbulence intensities, can have a significant effect on turbine operation via increased load magnitudes and fatigue. Accurate modelling of wind farm performance and turbine loading thus requires these effects to be taken into account. The ability to model multiple turbines operating in transient wind conditions also allows testing of wind turbine controllers and farm performance analysis.

The methods presented in this paper, develop those by Norris et. al. [4, 5] to include both a wind direction change or 'shift', and a combined gust and shift event. Wind turbine operation is modelled using an actuator technique and a coupling framework to model independently controlled turbines [7]. Large eddy simulation (LES) has been used to allow the resolution of transient turbulence structures. A regular grid of turbines, typical of an offshore wind farm is constructed and the latter sections describe the wind event structures generated by the models and the response of the wind turbine array.

2. Methodology

2.1. Flow Solver

The SnS CFD code developed at the University of Sydney and the University of Auckland [8, 9] uses a structured, non-staggered mesh and a fractional step solver for modelling transient flows [10]. Large-eddy simulation (LES) has been implemented with the Smagorinsky Sub-Grid Scale (SGS) model [11] to allow the modelling of high Reynolds number flows such as the atmospheric boundary layer. Wall effects are included with the near wall damping model of Mason and Thompson [12] and a rough wall function [13].

The effect of the wind turbines on the flow is modelled using the Actuator Sector Method [14] developed by the authors. Similar to an actuator line method, the Actuator Sector Method resolves the effects of individual turbine blades while retaining the efficiency of conventional actuator disc methods. By resolving individual turbine blades, this method allows the simulation of span-wise variations in turbine rotor loading which can be significant in sheared and yawed flows. The forces on the turbine are calculated using the FAST wind turbine simulation code from NREL [15] coupled to the LES. The resultant forces on the fluid are then implemented as time-varying sources and sinks in the momentum equations solved by the CFD code. A complete description of the solution method is presented in a previous publication [7].

2.2. Turbine Modelling

The NREL 5MW research turbine has been selected for this study. This turbine type is a fictitious model based on various commercial prototypes, particularly the REpower 5M turbine, and is featured in various recent control studies [16]. The machine is a conventional three-bladed, upwind variable speed, variable-pitch turbine with a rotor diameter of 126m and a hub-height of 90m. The turbine reaches rated power at 11.4ms^{-1} and 12.1rpm, corresponding to a rated tip speed of 80ms^{-1} and a tip speed ratio of 7. Detailed specifications of the turbine and controller can be found in the NREL report by Jonkman et al. [17].

In this work the turbine operates with the standard baseline controller which modulates generator torque and collective blade pitch. A yaw controller has been implemented based on the baseline controller from the pre-design phase of the DOWEC6MW turbine [18]. This controller uses a 30s moving average of the wind direction to monitor yaw misalignment. The controller activates yaw actuators at a yaw error of 5° with yaw rate of 0.3°s^{-1} until the 2s moving average of yaw error is less than 0.5°.

2.3. Wind Event Modelling

The wind event models explored in this research are based on the International Wind Turbine Design Standard IEC61400-1:2005 [1], with the main focus on the extreme coherent gust structure (ECG) which includes a large velocity increase accompanied by a simultaneous wind direction change. This structure poses a challenging modelling problem, and was selected to evaluate the feasibility of the technique for simulating large length-scale transient wind conditions. The models and simulations presented are applied to turbines operating in an offshore environment, although the methods can equally be applied to turbines operating in flat open terrain.

The approach for introducing wind event structures into the CFD domain was to develop transient boundary conditions to generate changes in the wind environment. Particular care was taken to ensure

the construction of a consistent set of boundary conditions for the simulation. The models developed below approach the two components of ECG, the gust structure and the wind shift structure separately. The assumption is made that the two structures can be linearly superimposed at the domain inlet to produce the combined wind event. The superposition process is simplified by modelling the two wind structures as span-wise periodic.

2.3.1. Gust Model For a wind event such as a gust entering the domain, the naïve procedure would be to simply increase the velocity at the upstream boundary. However, the fluid is modelled as incompressible, and this, together with the constraints imposed by the finite size of the computational domain, place restrictions on this approach. By increasing the velocity at the upstream boundary, mass conservation and incompressibility require the flow velocity to instantaneously increase throughout the domain. The solution proposed by Norris et. al. [4, 5] is to implement an inlet condition that ensures the total mass flux at the upstream boundary does not increase when a gust enters the domain. This may be achieved by changing the shape of the inlet profile such that the velocity is locally increased within the gust, with a corresponding decrease in flow across the rest of the inlet.

The gust perturbation has been implemented by modifying a base velocity profile, which includes turbulent fluctuations generated using Mann's Method [2]. The inlet condition can then be decomposed into components given by,

$$u(y,z,t) = u_b(y) + u_{trans}(y,z,t), \quad \text{and} \tag{1}$$

$$u_{trans}(y,z,t) = u'(y,z,t) + u_g(y,t) + u_{gc}(y,t), \tag{2}$$

where u is the stream-wise velocity, $u_b(y)$ is the base inlet velocity profile, $u'(y,z,t)$ represents the instantaneous turbulent fluctuations, $u_g(y,t)$ is the gust perturbation, and $u_{gc}(y,t)$ is a correction added to the inlet velocity profile. y is the elevation above the ocean surface, and z is the cross-flow direction. The vertical and lateral components of velocity are also given by v and w respectively.

Both the gust and turbulence perturbations added to the velocity profile are scaled such that,

$$\int_z \int_y u' dy dz = 0, \quad \text{and} \quad \int_z \int_y (u_g + u_{gc}) dy dz = 0, \tag{3}$$

to enforce a constant mass flux at the inlet.

The gust perturbation profile $u_g(y,t)$ in this study was based on the ECG defined in the Wind Turbine Design Standard.

$$u_g(y,t) = U_g u_g(y) u_g(t), \tag{4}$$

where U_g is the magnitude of the gust relative to the base velocity profile.

The profile of the standard gust velocity is simply a uniform increase in velocity over the turbine rotor. A suitable profile is given by,

$$\frac{u_g(y)}{U_g} = \text{erf}\left(\frac{\varepsilon y}{2\alpha}\right), \tag{5}$$

where an error function has been used to ensure consistency with a no-slip wall condition at the lower domain boundary. Here, $\varepsilon = 2.0\,\text{erf}^{-1}(0.99)$ (or the non-dimensional 99% extent of an error function), and α is a height threshold, typically the lower limit of the turbine rotor.

A correction profile is used to maintain the uniform increase in velocity over the turbine rotor. A suitable profile is given by,

$$\frac{u_{gc}(y,t)}{U_c(t)} = \left(\text{erf}\left[\frac{\varepsilon\,(y-\beta)}{\delta_g}\right] - 1\right), \tag{6}$$

where $U_c(t)$ is the amplitude scaling factor used for mass flux correction, β is a height threshold, typically the height of the turbine rotor apex, and δ_g is a scaling factor for the extent of the error function ramp. This value represents the height of the shear layer above the gust region and determines in part, both the size of the final gust region and the extent of the vorticity generated in the shear layer. In this work, δ_g was set to $2D$.

The factor $U_c(t)$ is used to scale the correction and maintain the mass flux at the inlet.

The variation in gust strength with time is given by $u_g(t)$. For the current model this has been defined using the piece-wise inverted cosine from ECG standard given by,

$$\frac{u_g(t)}{U_g} = \begin{cases} 0 & : t < 0 \\ 0.5(1-\cos(\pi t/T_{gr})) & : 0 \le t \le T_{gr} \\ 0 & : t > T_{gr} \end{cases} . \tag{7}$$

Examples of the non-dimensionalised gust velocity profile and correction are illustrated in Figure 1, along with a time trace of amplitude, where H is the hub-height of the turbine.

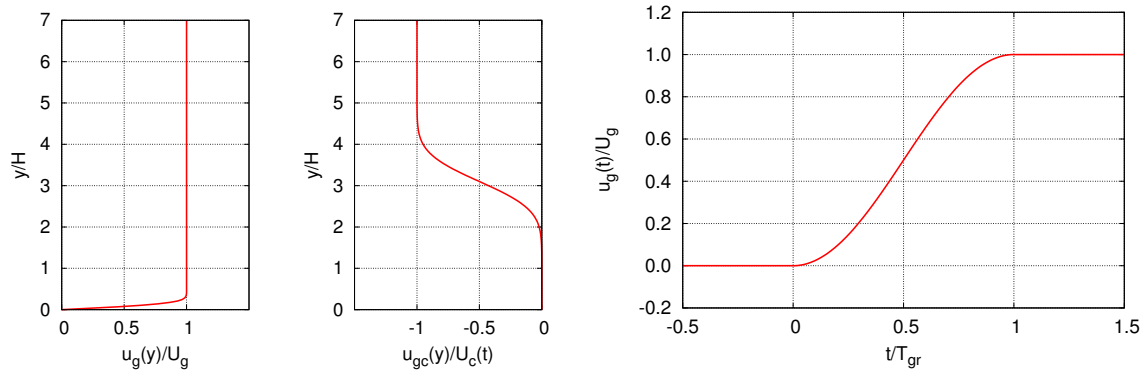

(a) (b) (c)

Figure 1. (a) The vertical gust velocity profile given by Eq. 5. (b) The vertical gust correction profile given by Eq. 6. (c) The variation gust velocity with time given by Eq. 7

2.3.2. Wind Shift Model In addition to the gust model, a method for modelling a wind direction change is also required. The objective is to model a wind direction change that propagates through the domain. The proposed solution is to introduce a lateral component of velocity gradually along the domain sides. Periodic lateral boundary conditions can be exploited by introducing a lateral component of velocity to the velocity profile at the inlet. This produces a shift front, perpendicular to the inlet, which propagates through the domain at the free-stream wind speed.

According to the IEC standard, the wind shift angle θ transient is determined using the same inverted cosine function as the gust transient, given by,

$$\theta(t) = \begin{cases} 0 & : t < 0 \\ 0.5(1-\cos(\pi t/T_{sr})) & : 0 \le t \le T_{sr} \\ 0 & : t > T_{sr} \end{cases} , \tag{8}$$

where the parameter T_{sr} governs the rise-time of the direction change.

The relationships of the stream-wise and lateral components of velocity (u and w respectively) to the wind direction angle are given by,

$$u_s(y,\theta) = -u_b(y)((1-cos(\theta)), \quad \text{and} \tag{9}$$

$$w_s(y,\theta) = u_b(y)\sin(\theta). \tag{10}$$

The w velocity component profile has the same form as the u base profile to maintain a constant direction change with elevation. A change in the u velocity is required to maintain the velocity magnitude throughout the direction change.

The resulting stream-wise and lateral velocity components at the inlet are given by,

$$u(y,z,t) = u_b(y) + u'(y,z,t) + u_s(y,t) + u_{sc}(y,t), \quad \text{and} \tag{11}$$

$$w(y,z,t) = w'(y,z,t) + w_s(y,t), \tag{12}$$

respectively, where u' and w' are the instantaneous turbulent velocity fluctuations. The term, $u_{sc}(y,t)$ is a correction included to adjust for changes in the stream-wise mass-flow rate through the domain. This correction can either increase or reduce velocities in the upper section of the profile to conserve the mass-flow rate depending on the initial and final wind directions. Similar to the gust model, a suitable correction profile is given by,

$$u_{sc}(y,t) = U_{sc}(t)\left(\text{erf}\left[\frac{\varepsilon\,(y-\beta)}{\delta_s}\right] - 1\right), \tag{13}$$

where $U_{sc}(t)$ is a scaling factor, β is an elevation threshold similar to that used in the gust model, and δ_s is a scaling factor for the extent of the error function ramp. Typically, the mass flux change during the shift is much smaller than that observed in the gust model. In some cases δ_s can be greater than δ_g to reduce the velocity gradient introduced by the correction.

2.4. Computational Domain & Boundary Conditions

A cuboidal flow domain was constructed to model three rows of wind turbines operating in a grid arrangement. Offshore conditions were simulated with the turbines operating in a stable, non-stratified, turbulent boundary layer over open sea. The configuration of the computational domain including the wind turbine array is shown in Figure 2.

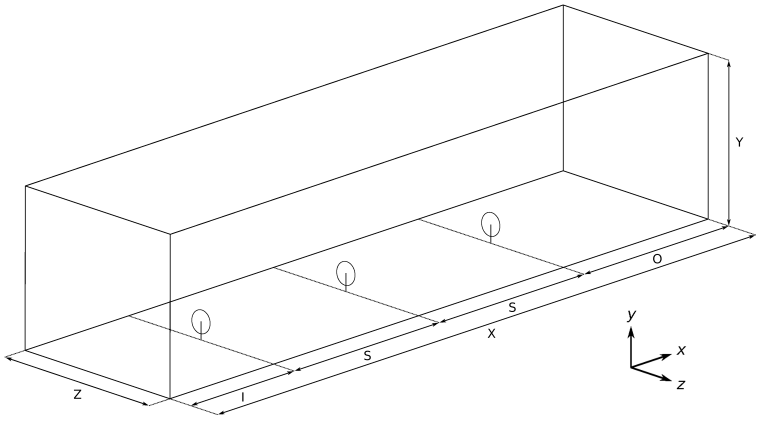

Figure 2. The computational domain showing the wind turbine array. X, Y and Z are the dimensions of the domain. I is the distance from the inlet to the first turbine. S is the spacing between turbines and O is the distance from the last turbine to the outlet. Periodic boundaries are defined in the z direction.

A structured Cartesian mesh was created which works efficiently in conjunction with the solver utilised in this research. Local refinement was made in the lower region of the domain which includes the turbine rotors and wake regions. The total number of mesh cells in the domain was 70.6×10^6 with a constant mesh size in the refined regions of 3.0m^3. This corresponds to 42 cells per rotor diameter, or ≈ 1375 cells over the rotor swept area. Previous work by the authors have shown this mesh size gives adequate resolution of the turbine rotor aerodynamics and wake structures[19]. All spacings and length measurements were non-dimensionalised by the turbine rotor diameter of $D = 126\text{m}$. The domain measured $(26D \times 12D \times 7D)$ in the x, y and z directions respectively, with the first turbine located at $I = 5D$ from the inlet boundary and centred in the z direction. The rotor hub height was $H = 90\text{m}$ as defined in the turbine specification. The spacing S between the turbines was set to $7D$ in the stream-wise direction as well as the y direction by imposing periodic boundary conditions on the two side-walls. The turbine rows are therefore located at $5D$, $12D$ and $19D$ from the inlet for rows 1 through 3 respectively.

A power law profile with turbulent fluctuations simulates the turbulent atmospheric boundary layer at the inlet. The shear exponent of the profile is defined in the IEC61400-3:2009 standard for offshore turbines as 0.14[20]. An outlet condition with a prescribed pressure was applied at the downstream

boundary. The lower domain boundary was implemented using a rough-wall condition with an effective roughness height of 2.46×10^{-4}m to simulate a flow over open water. This roughness length is derived iteratively from the Charnock expression also specified in the IEC61400-3:2009 standard. A symmetry condition was specified at the top boundary. With the use of LES, periodic lateral boundary have been employed to avoid damping of the turbulence field, and to allow the wind shift.

A reference wind speed of $U_{ref} = 15\text{ms}^{-1}$ was chosen for the simulations. This is above rated speed for the NREL5MW turbine and corresponds to 1.5 times average wind speed for a class 1B turbine as defined in the IEC61400-1:2005 standard. The 1B classification is typical for turbines located offshore. The Mann uniform shear turbulence model from the standard was used to generate a set of turbulent fluctuations with a turbulence intensity 9.5% at the domain inlet. The parameters of the gust structure entering the domain are those defined in the standard with the rise time, $T_{gr} = 10.5$ seconds, and the gust magnitude, $U_g = 15.0\text{ms}^{-1}$. Similarly for the wind shift, the shift magnitude for $U_{ref} = 15\text{ms}^{-1}$ is defined as 48°. The shift rise time is governed by the same transient as the gust.

2.5. Blade Loads & Bending Moments

Individual turbine blade root bending moments, both in-plane (IPBM) and out-of-plane (OoPBM) as well as the fore-aft tower base bending moment (TBBM) were obtained from the coupled FAST aero-elastic solver. The 5MW turbine model used has all of the degrees of freedom associated with flexibility turned off which makes this calculation relatively straightforward. However, the tower bending moment calculated does take into account the moving centroid of the blade loads. The associated Damage Equivalent Load (DEL) calculations are based on the mean bending moments of turbine 1 during the steady period before arrival of the ECG, and uses three times the maximum bending moment recorded during the entire run as the ultimate load case. A slope index, m = 10 was selected for fibre laminate constructions (i.e. the blades) and m = 2 for steel structures (i.e. the tower). These values and the DEL calculation procedure are provided in an NREL technical report [21].

3. Results and Discussion

Results are presented for the combined ECG structure moving through an array of turbines. All the results have been presented in terms of a non-dimensionalised time τ_s, given by,

$$\tau_s = \frac{tU_{ref}}{D}, \tag{14}$$

where t is the simulation time. τ_s represents the time for a fluid element travelling at U_{ref} to convect a distance of $1D$. $\tau_s = 0$ is the time at which the wind structure enters the domain.

Initially, simulations were conducted where the gust and shift models were implemented separately in order to verify the operation of the models and investigate the propagation of the wind event structures. Although these simulations are not presented in this paper, results from this work have been used to determine a time delay of $2\tau_s$ to coordinate the arrival of the gust and shift at the initial turbine location.

In order to minimise the change in u_s, and the corresponding mass-flow correction during the wind shift, an initial wind angle of $\theta_0 = -24^\circ$ was selected, with a direction change of $\theta_s = 48^\circ$. The wind direction is then given by $\theta = \theta_0 + \theta_s$, with a final wind direction of 24°.

A time-series of velocity magnitude is shown in Figure 3(a) with the time delay evident in the inlet data. A maximum velocity magnitude of $2U_{ref}$ is observed as expected.

The gust magnitude is shown to decay along the domain, with peak gust velocities of approximately 0.9, 0.8 & $0.8U_{ref}$ for the first through third turbine rows respectively. This decay in gust magnitude is expected due to turbulent mixing in the boundary layer and momentum lost to the wind turbine which act as momentum sinks.As the turbine locations are aligned with the domain rather than initial wind direction, subsequent turbines are not affected by the wake of the turbines directly upstream. However, the third turbine row does exhibit evidence of increased turbulence levels due to the wake from the first turbine row due to the periodic boundary condition.

Figure 3(b) illustrates the change in wind direction at the turbine locations. The changes in wind direction correspond well with the arrival of the gust front, indicated in Figure 3(a), demonstrating that

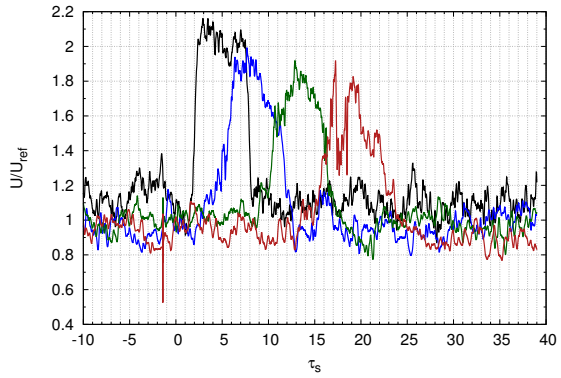

(a) A time-series of the hub-height velocity magnitude at various locations in the domain starting with the inlet (black), followed by the first through third turbine hub locations indicated in blue, green and red.

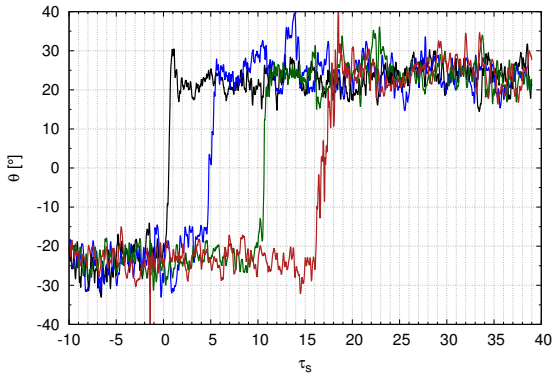

(b) A time-series of the hub-height wind direction in the domain starting with the inlet (black), followed by the three turbine hub locations.

Figure 3. Wind speed and direction during an ECG.

the two ECG components can be coordinated at the turbine locations. The ECG front arrives at the initial turbine location at $\tau_s \approx 4$. At locations downwind of the initial turbine, the normalised time delay between the arrival of the front is $\approx 5\tau_s$. This is less than the reference velocity time-delay of $7\tau_s$ (corresponding to the turbine spacing of $7D$), indicating that the structure has a group velocity of $\approx 1.2U_{ref}$.

The variation of pitch actuation for the three turbine rows is shown in Figure 4(a). Increases in pitch actuation reflect the arrival of the gust front and the subsequent saturation of aerodynamic power. The associated yaw error is shown in Figure 4(b) where peaks in yaw error are observed to trigger yaw actuation of the turbines. The maximum yaw error recorded is observed at turbine 3. This increase is due to the large amount of turbulent mixing associated with both the *uv* and *uw* shear components.

The bending moment data during the ECG are shown in Figure 5. Time history data for successive turbines show that loads decrease initially with large pitch actuation and then increase once the gust front has passed. At this point the turbine remains operating with a high yaw error. The variation between the responses of the turbine rows during the extreme wind conditions demonstrates the significance of modelling the transformation of wind event structures and wind turbine wake effects.

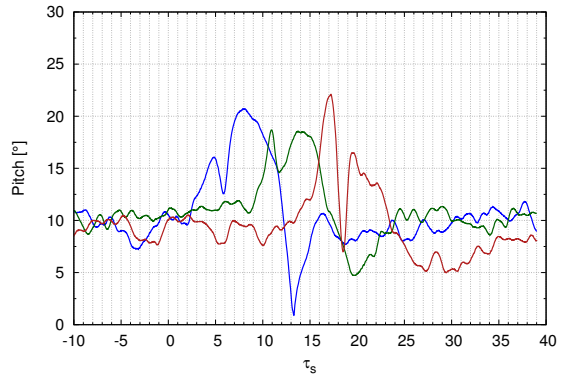

(a) A time-series of wind turbine pitch position for the first through third turbine hub locations indicated in blue, green and red.

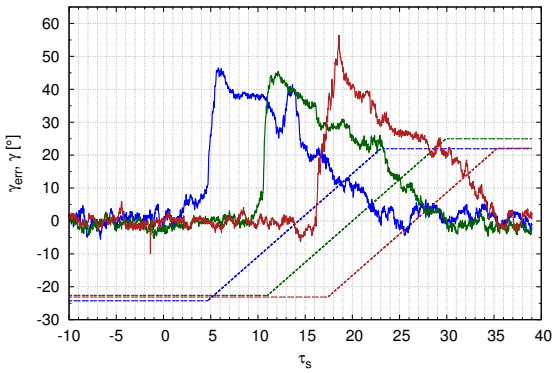

(b) A time-series of nacelle yaw error γ_{err} (solid) and nacelle yaw angle γ (dashed) for the first through third turbine hub locations.

Figure 4. Turbine pitch and yaw angles during an ECG.

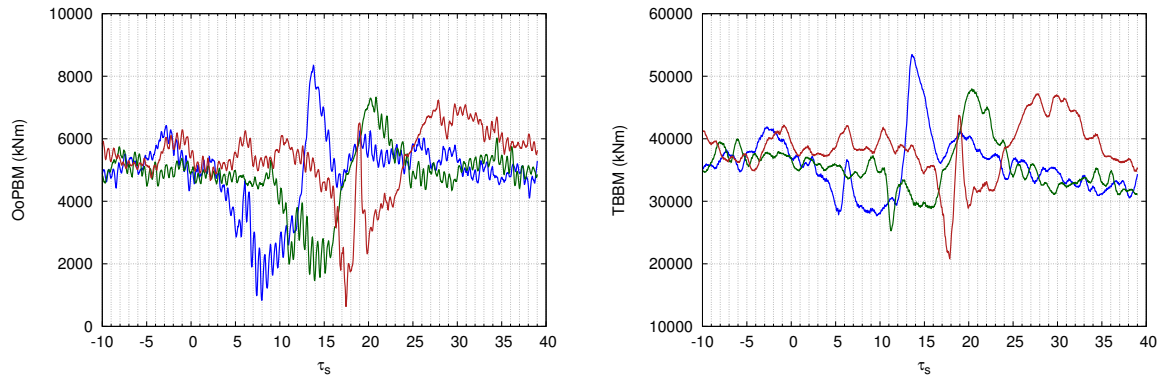

(a) A time-series of out-of-plane bending moment for the first through third turbine hub locations indicated in blue, green and red.

(b) A time-series of tower bending moment for the first through third turbine hub locations.

Figure 5. Bending moments during an ECG.

Table 1 shows the damage equivalent loads for the tower, in-plane and out-of-plane bending moments, in the period before and during the wind event for each turbine. The DELs are calculated for a fixed width window of 25 τ_s, which is shifted to cover the ECG wind event and the transient response of each turbine. An comparative DEL using the same time window is also calculated for each turbine prior to the arrival of the ECG. For example, the DEL windows for turbine 1 cover -25 τ_s to 0 τ_s, and 2 τ_s to 27 τ_s.

Table 1. Normalised Time-Averaged Damage Equivalent Loads for 3 Turbines

	Pre-ECG Event			During ECG Event		
	Tower	In-Plane	Out-of-Plane	Tower	In-Plane	Out-of-Plane
Turbine 1	1.00	1.00	1.00	1.38	1.05	2.15
Turbine 2	0.85	0.99	0.90	1.08	1.05	1.75
Turbine 3	0.82	0.94	0.85	1.31	1.04	2.14

A reduction in out-of-plane bending moment and tower bending moment DEL at downwind locations is observed before the introduction of the ECG due to the decay in turbulence intensity through the domain. This decay is unexpected and occurs despite the implementation of the wall roughness length scale according to the IEC standard recommendations for offshore turbulence.

During the event, the data show that tower and out-of-plane bending moment DEL are most affected by the ECG. The largest increase in DEL is for the tower bending moment at turbine 3; this is likely to be due to the generation of high intensity turbulent structures at the ECG front. The observed trend in the tower bending moment DEL corresponds to the trend in maximum yaw error. There are increases in out-of-plane blade bending moment DEL of 115%, 94%, and 152% for turbine locations 1 through 3 respectively. Again, the largest increase is at the most downstream turbine location. This is the result of a combination of wake effects and high levels of turbulence due to mixing at the ECG front. In-plane loadings do not show significant changes in behaviour; this is as expected as overall rotor torque and power are maintained at the rated values for all the turbines throughout the wind event, since aerodynamic power is regulated by blade pitch for this turbine.

4. Conclusions

A methodology for implementing both an extreme gust model and extreme wind shift model from the IEC turbine design standard in a CFD flow domain has been described and applied to the flow through an array of wind turbines. A combined extreme coherent gust structure has been implemented by superimposing

the gust and shift structures at the domain inlet with an appropriate time delay to coordinate the arrival of the wind event at the successive turbine locations. It is demonstrated that significant pitch actuation occurs in the wind turbine array to control the turbine power output as the high velocity front propagates through the turbine locations. Large yaw errors associated with rapid wind direction change trigger yaw actuation of the turbines. The effect of the ECG event on the blade and tower loads has been observed. It has been shown that wake turbulence can have a significant effect on turbine fatigue loading in transient atmospheric conditions. Simulating the propagation of the wind events is significant due to the high levels of turbulence at the wind event front, which change the character of an extreme event as it passes through a turbine array. These simulations demonstrate the ability to successfully model multiple turbines operating with baseline controllers in highly transient atmospheric conditions. This method allows the analysis of overall wind farm performance and the ability to investigate novel turbine controllers and wind farm scale control strategies.

Acknowledgements

The authors would like to acknowledge the funding of a University of Auckland Doctoral Scholarship. The contributions to the CFD code by S. Armfield from The University of Sydney are greatly appreciated. New Zealand's national computing facilities are provided by the NZ eScience Infrastructure (NeSI). The authors wish to acknowledge the contribution of the NeSI facilities to the results of this research. URL http://www.nesi.org.nz.

References

[1] *IEC61400-1:2005, Wind turbines - Part 1: Design requirements*, 2006.
[2] J. Mann. Wind field simulation. *Probabilistic Engineering Mechanics*, 13(4):269–282, 1998.
[3] D. J. Laino and A. C. Hansen. User's guide to the wind turbine aerodynamics computer software AeroDyn. Technical report, NREL, 2002.
[4] S. E. Norris, J. E. Cater, K. A. Stol, and C. P. Unsworth. Wind turbine wake modelling using Large Eddy Simulation. In *Proceedings of the 17th Australasian Fluid Mechanics Conference*. University of Auckland, December 2010.
[5] S. E. Norris, R. C. Storey, K. A. Stol, and J. E. Cater. Modeling gusts moving through wind farms. In *Proceedings of the 31st Wind Energy Symposium*. AIAA, 2012.
[6] E. Hau. *Wind Turbines: Fundamentals, Technologies, Applications, Economics*. Springer, Oxford, 2006.
[7] R. C. Storey, S. E. Norris, K. A. Stol, and J. E. Cater. Large eddy simulation of dynamically controlled wind turbines in an offshore environment. *Wind Energy*, 2012.
[8] S. W. Armfield, S. E. Norris, P. Morgan, and R. Street. A parallel non-staggered Navier-Stokes solver implemented on a workstation cluster. In *Computational Fluid Dynamics 2002: ICCFD2*, pages 30–45, 2003.
[9] S. E. Norris. *A Parallel Navier–Stokes Solver for Natural Convection and Free Surface Flow*. PhD thesis, University of Sydney, 2000.
[10] S. W. Armfield and R. Street. An analysis and comparison of the time accuracy of fractional-step methods for the Navier-Stokes equations on staggered grids. *International Journal for Numerical Methods in Fluids*, 38:255–282, 2002.
[11] J. Smagorinsky. General circulation experiments with the primitive equations. *Monthly Weather Review*, 91(3):99–164, 1963.
[12] P.J. Mason and D.J.Thomson. Stochastic backscatter in large-eddy simulations of boundary layers. *J. Fluid Mech.*, 242:51–78, 1992.
[13] P.J. Mason and N.S. Callen. On the magnitude of the subgrid-scale eddy coefficient in large-eddy simulations of turbulent channel flow. *J. Fluid Mech.*, 162:439–462, 1986.
[14] R. C. Storey, S. E. Norris, and J. E. Cater. An actuator sector method for efficient transient wind turbine simulation. *Wind Energy*, 2014.
[15] J. M. Jonkman and M. L. Buhl Jr. FAST User's Guide. Technical report, National Renewable Energy Laboratory, 2005.
[16] M. Spencer, K. A. Stol, and J. E. Cater. Predictive yaw control of a 5mw wind turbine. In *Proceedings of the 31st Wind Energy Symposium*. AIAA, 2012.
[17] J. Jonkman, S. Butterfield, W. Musial, and G. Scott. Definition of a 5-MW reference wind turbine for offshore system development. Technical report, National Renewable Energy Laboratory, 2009.
[18] H. J. T. Kooijmann, C. Lindburg, D. Winkelaar, and E. L. van der Hooft. Dowec 6MW pre-design: Aero-elastic modelling of the dowec 6MW pre-design in phatas. Technical report, Energy Research Center of the Netherlands (ECN), 2003.
[19] M. P. van der Laan, R. C. Storey, N. N. Sørensen, S. E. Norris, and J. E. Cater. A CFD code comparison of wind turbine wakes. Submitted to: The Science of Making Torque from Wind, June 2014.
[20] *IEC61400-3:2009, Wind turbines - Part 3: Design requirements for offshore wind turbines*, 2009.
[21] G. Freebury and W. Musial. Determining equivalent damage loading for full-scale wind turbine blade fatigue tests. Technical report, National Renewable Energy Laboratory, 2009.